Electronic Supplementary Material (ESI) for Integrative Biology

Supplementary Information

Stabilization effects of fibroblasts on endothelial sprouting

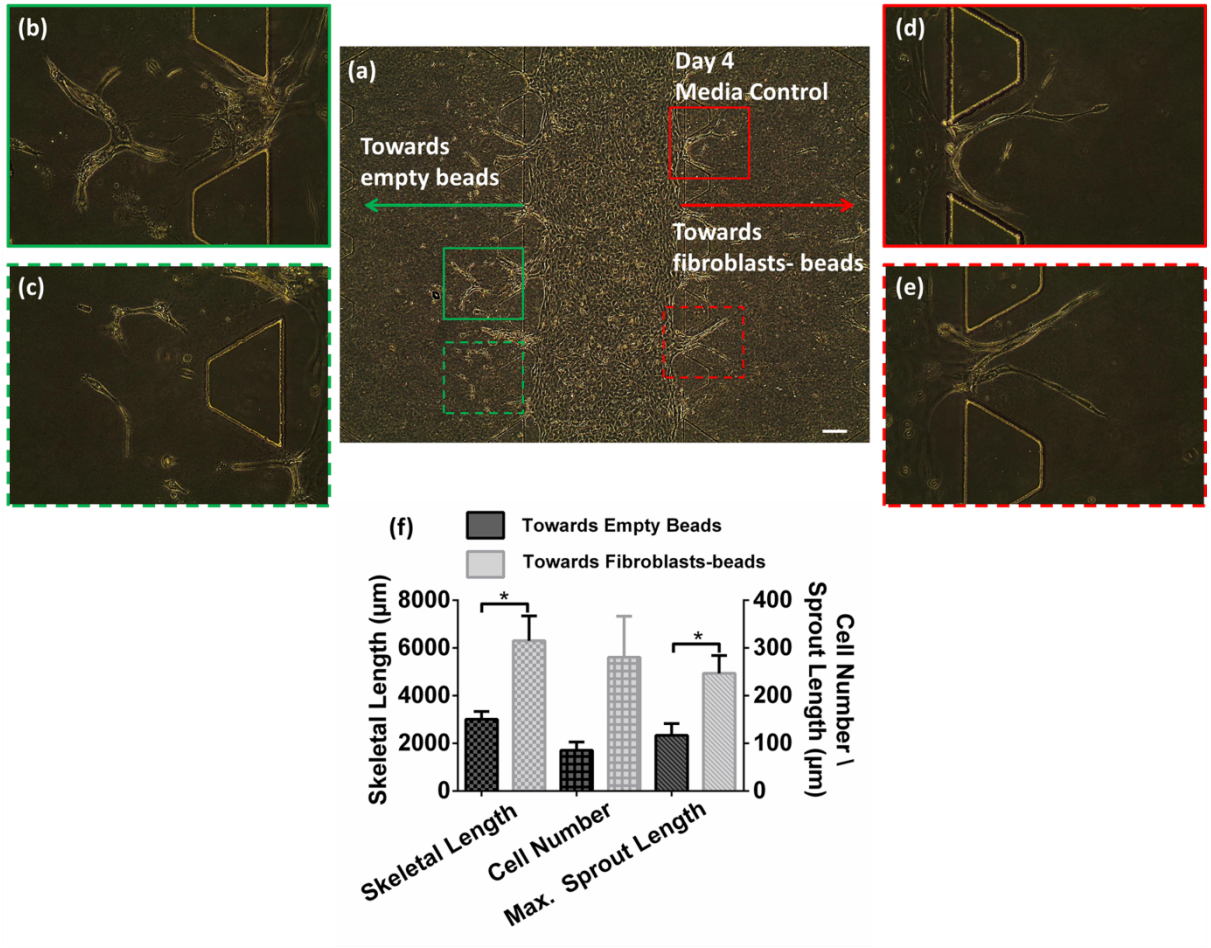

Fig. 9 Fibroblasts induce and stabilize endothelial sprouting in collagen gel. (a) 4x phase contrast image of endothelial cells sprouting assay in cell culture media at day 4. (b) and (c) 20x phase contrast images of detached sprouts and endothelial cells from the EC monolayer that were growing towards empty alginate beads. (d) and (e) 20X phase contrast images of sprouts growing towards fibroblast-encapsulated alginate beads. (f) Quantification of skeletal length, cell number and maximum sprout length for sprouts growing towards empty beads and towards fibroblast-encapsulated beads in cell culture media. Without the support of fibroblasts, sprouts would regress or detach from EC monolayer on day 4. Scale = 100 µm. * $p < 0.05$

Sprouts formed under the induction of CPX + S1P

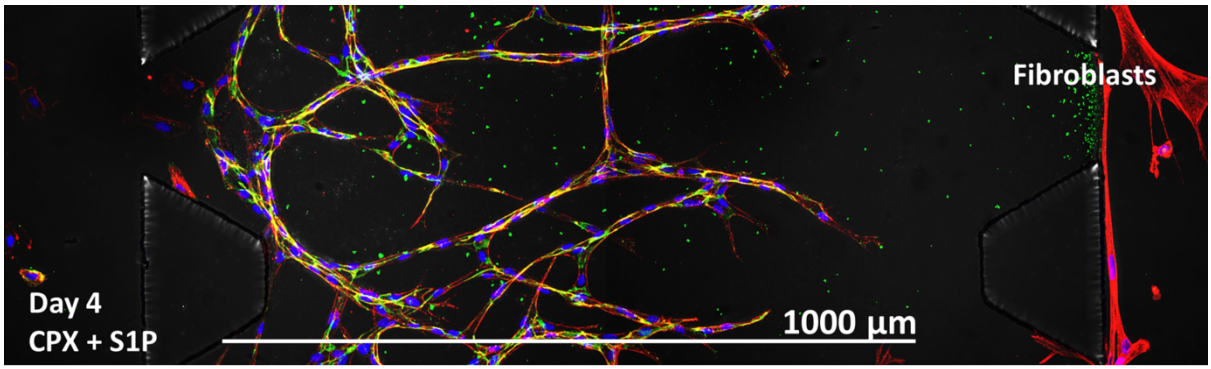

Fig. 10 Sprouts formed under the induction of CPX + S1P extended three quarters of the way across the collagen region. Stitched 20 X confocal images with Hoechst stained nuclei (blue), rhodamine phalloidin stained actin (red) and Alexa fluor 488 immunostained VE-cadherin (green) show that sprouts grew and extended around 800 µm into collagen gel in 4 days under the influence of CPX and S1P. Scale bar = 1000 µm.

CPX stabilized HIF-1α

We did immunofluorescent staining to confirm that CPX stabilizes HIF-1α in normoxia. The figure below demonstrates that CPX or CPX in combination with S1P prevent HIF-1α from degradation as compared to media control group or S1P treated group in fibroblasts culture. The western blot results further confirm that CPX stabilized HIF-1α *in vitro*.

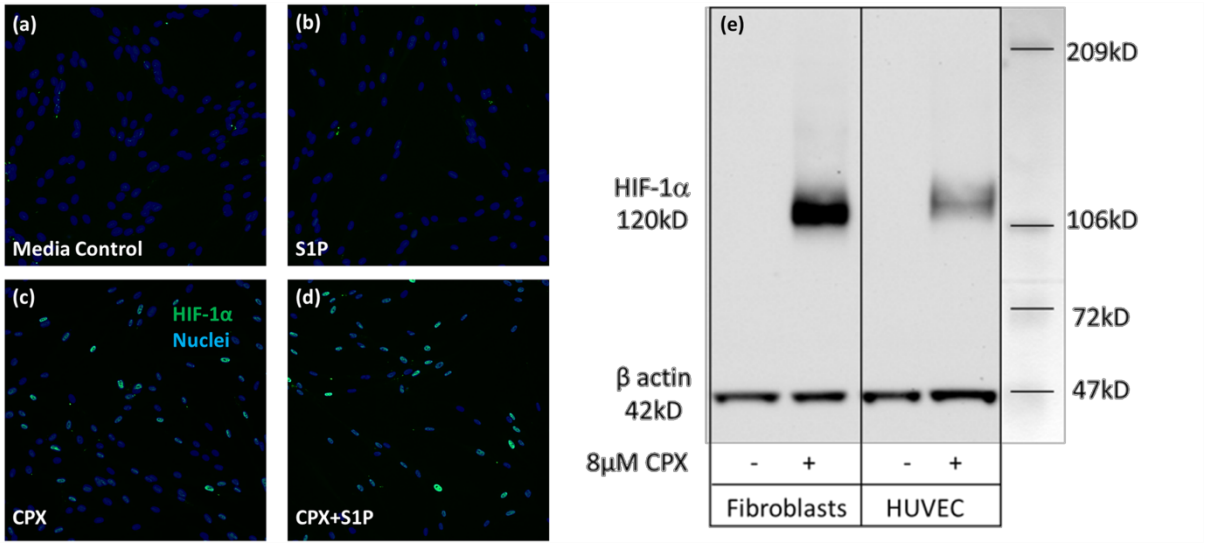

Fig. 11 CPX prevents the degradation of HIF-1α. (a) – (d) 4x fluorescent image of fibroblasts with Hoechst stained nuclei (blue) and Alexa fluor 488 immunostained VE-cadherin (green) under different pharmacological inductions. (e) Immunoblot was stained with antibodies against HIF-1α and β actin to detect HIF-1α in fibroblasts and endothelial cell lysate with CPX treatment.

Hydralazine hydrochloride (HDZ) induced angiogenesis in microfluidics

We studied the effects of another PHi which is also an iron chelator, hydralazine hydrochloride (HDZ). As shown in the figure below, HDZ elicited angiogenesis in similar settings but not as intensive as CPX. Therefore, CPX was chosen for our study.

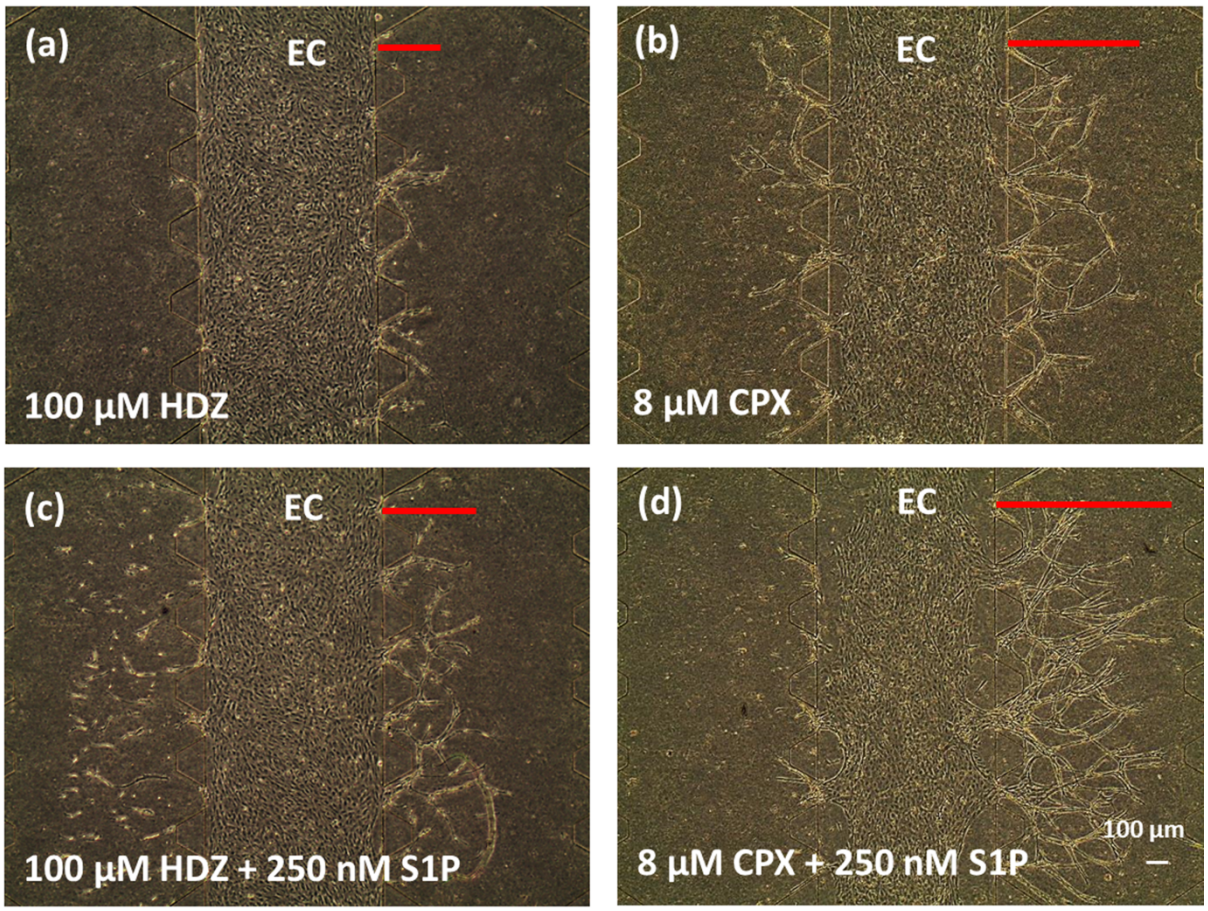

Fig. 12 Different PHis show differential angiogenic potentials. (a) – (b) Phase contrast images of 100 µM HDZ and 8 µM CPX induced angiogenesis in collagen that is adjacent to the fibroblasts encapsulated alginate beads in right channel. (c) – (e) Phase contrast images of endothelial sprouting under the induction of S1P combined with HDZ and CPX respectively. CPX outperforms HDZ in inducing angiogenesis in *in vitro* microfluidic assay, regardless of being applied individually or in combination with S1P. Red bars denote approximate length of sprouts. Scale bar = 100 µm.

CPX induces secretion of complementary angiogenic proteins from both fibroblasts and endothelial cells

With treatment of CPX alone or CPX + S1P, EC showed increased secretion of placental growth factor (PlGF), endothelin-1, epidermal growth factor and interleukin-8, fibroblasts upregulated secretion of hepatocyte growth factor, insulin-like growth factor-binding protein 2, urokinase plasminogen activator and most importantly, vascular endothelial growth factor (VEGF) among the 55 angiogenesis related proteins that the proteome profiler can detect. No significant increase in proteomic secretions were observed with S1P only. The data were validated through ELISA assay. We found that CPX + S1P can increase the PlGF secretion rate in endothelia from 765 ± 37.1 (± SE) to 3300 ± 631 pg/ml-Million cell-day while S1P did not show any significant effect. In fibroblasts we confirmed an increase of VEGF secretion from 280 ± 59.6 to 2080 ± 60.3 pg/ml-Million cell-day.

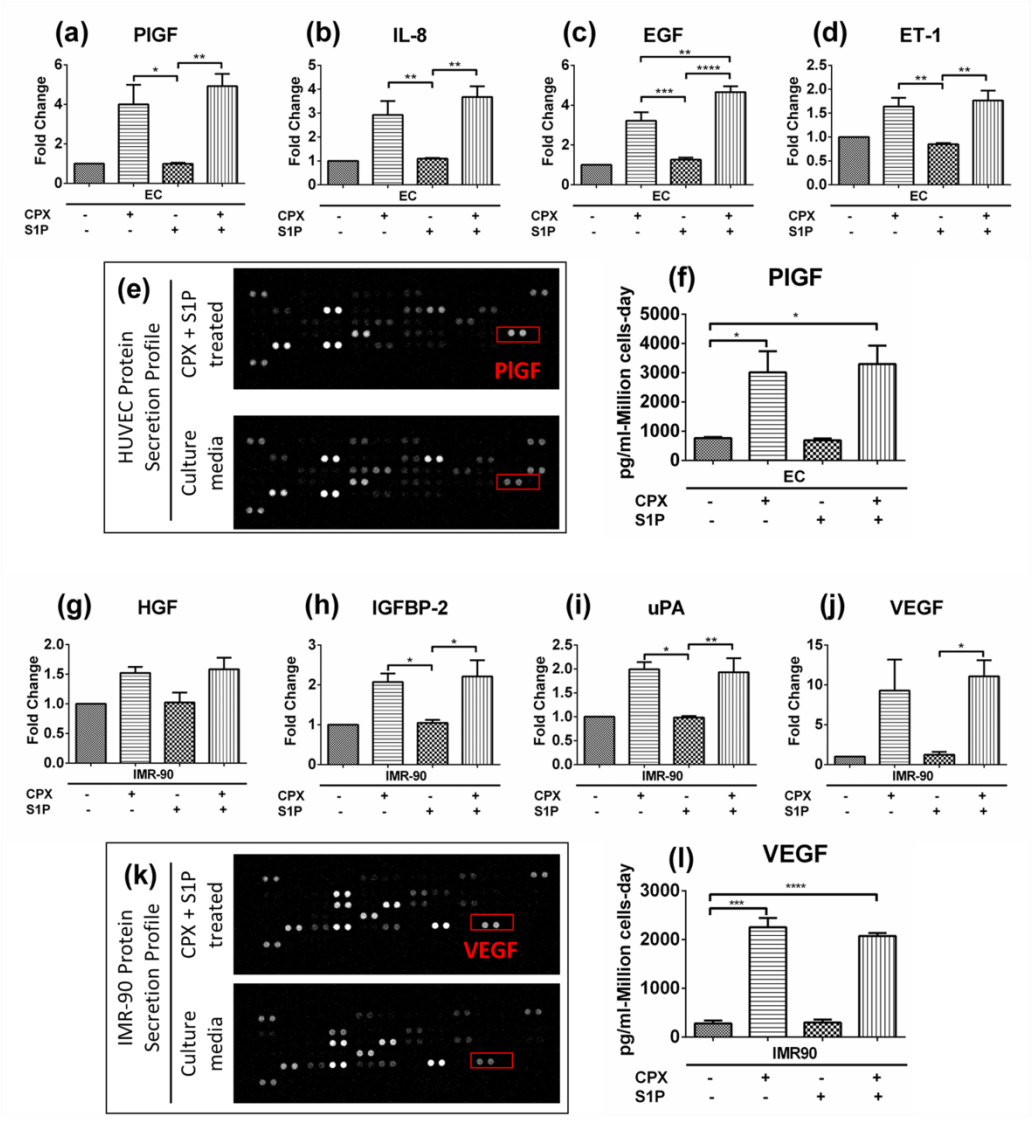

Fig. 13 CPX induces secretion of different angiogenic proteins by endothelial cells and fibroblasts. (a-d): proteomic analysis plots of proteins upregulated in HUVEC treated with CPX + S1P. The upregulated proteins are PlGF (4.9x), IL-8 (3.7x), EGF (4.7x) and endothelin-1 (1.8x). CPX and S1P combination further increased EGF expression by 45 % as compared to CPX only. (g-j): proteomic analysis plots of proteins upregulated in IMR-90 fibroblasts treated with CPX + S1P. The upregulated proteins include HGF (1.6x), IGFBP-2 (2.2x), uPA (1.9x) and VEGF (11x). CPX appears to be the main compound causing the observed upregulation. (e) and (k): representative images of 3 proteomic profiler membranes showing differences in protein secretion between CPX and S1P treated group and non-treated group (culture media control). (f) and (l): ELISA quantitation of PlGF and VEGF corroborating semi-quantitative results shown in A-I where PlGF secretion was increased from 765 ± 37.1 (± SE) to 3300 ± 631 pg/ml-Million cell-day while VEGF was upregulated from 280 ± 59.6 to 2080 ± 60.3 pg/ml-Million cell-day. Fibroblasts were cultured in VEGF free media for ELISA quantification to obtain true secretion rate of VEGF by fibroblasts. Error bars denote SE. * $p < 0.05$

Exogenously added VEGF induced capillary sprouting

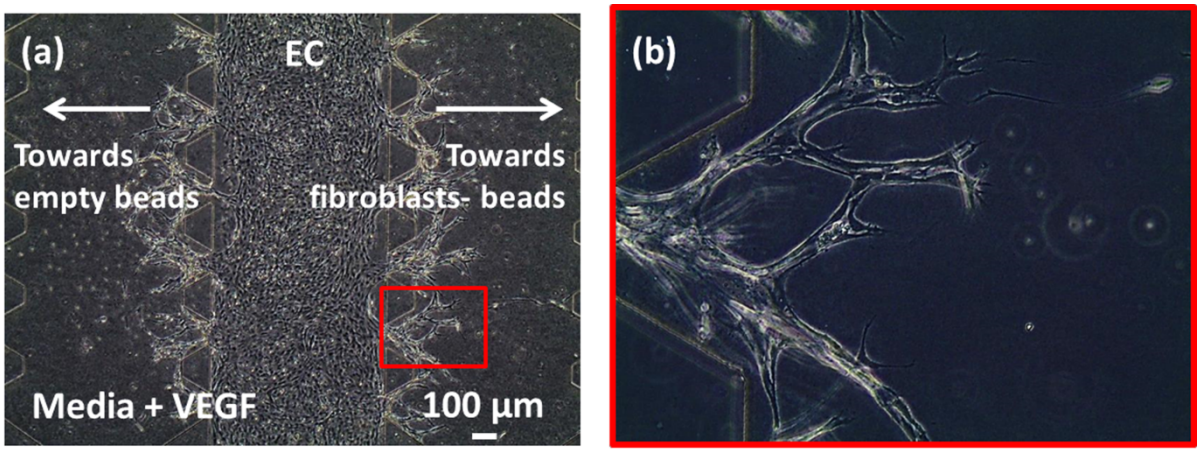

Fig. 14 VEGF induced capillary sprouting in 3D collagen gel. 4x Phase contrast image of VEGF induced capillary sprouting in 3D collagen gel. (b) Magnified image of specified area in (a) that showed the anastomosis of two nearby sprouts. Scale bar = 100 µm.

VEGF in culture media was depleted in EC culture within 24 h

The concentration of VEGF in EC culture was measured through ELISA assay to determine if VEGF would deplete in EC culture over 24 h. The concentrations of VEGF in both CPX + S1P treated and non-treated EC culture were measured at 8.66 ± 2.05 and 1.38 ± 0.69 pg/ml respectively which were drastically different from the VEGF concentration in media control that was measured at 1280 ± 16.0 pg/ml.

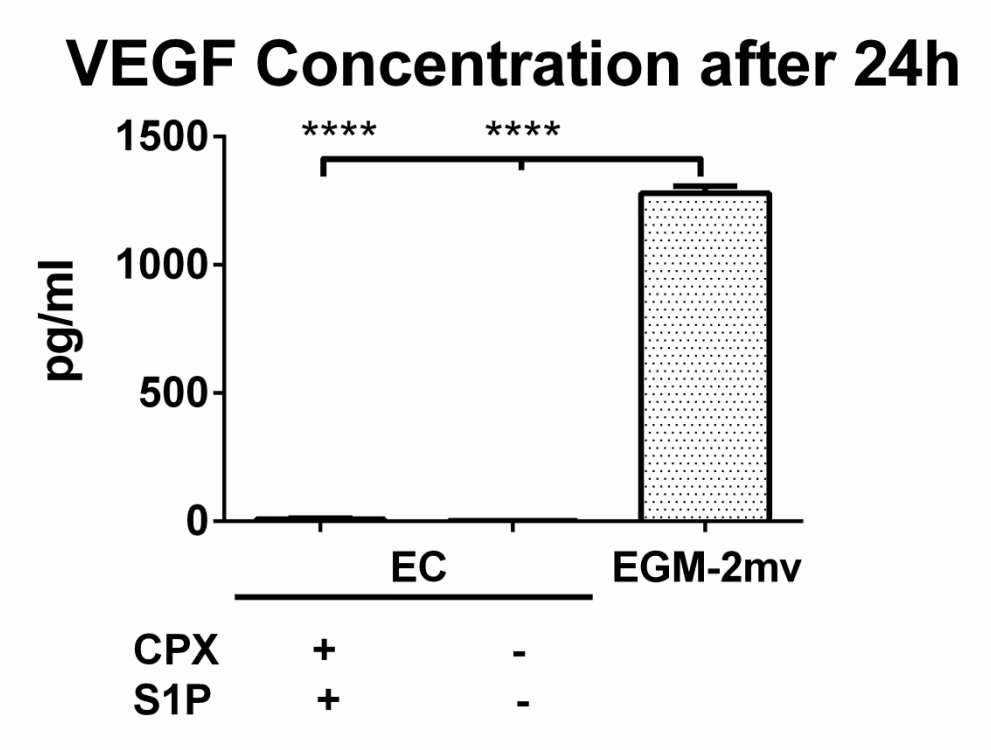

Fig. 15 Concentrations of VEGF in cell culture media in EC culture after 24 h. VEGF was depleted almost completely in culture media in EC culture after 24 h in both CPX + S1P treated and non-treated groups while the concentration of VEGF in media control was measured at 1280 ± 16.0 (± SE) pg/ml.

Angiogenic effects of S1P were mediated through $S1P_1$ receptor

$S1P_1$ receptor specific inhibitor, W146 was used to determine if S1P enhanced angiogenesis through $S1P_1$ in our settings. 10 µM of W146 effectively attenuated the sprouting response induced by CPX + S1P and reduced it to baseline levels. Although we observed negative effects on angiogenesis caused by equal volume of vehicle (ethanol), the inhibitory effects of W146 could still be clearly seen in terms of skeletal length of sprouts, the number of cells and the maximum length of sprouts.

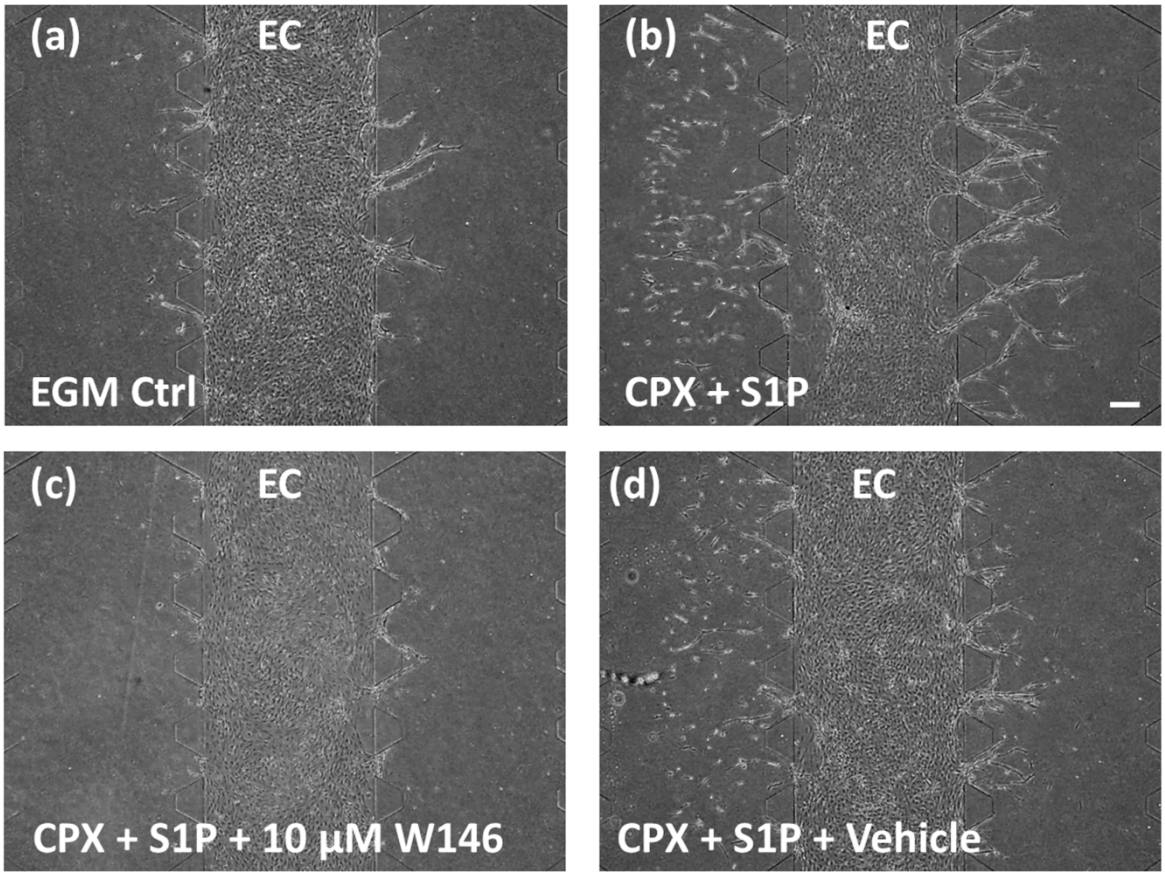

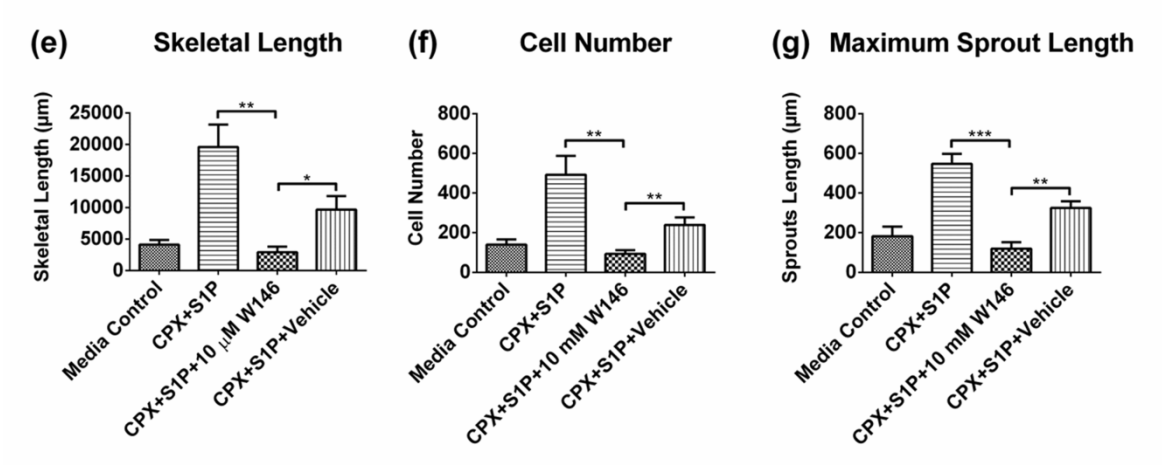

Fig. 16 $S1P_1$ specific inhibitor, W146 inhibits CPX and S1P induced angiogenesis. (a) - (d) 4X phase contrast images showed the inhibitory effects of W146 on CPX and S1P induced angiogenesis. (e) - (g) Quantifications of skeletal length, cell number and maximum sprout length. Attenuation effects of W146 on capillary sprouting were clearly seen in terms of shorter skeletal and maximum sprout length and reduced cell number despite of the negative effects caused by vehicle. Scale bar = 100 µm. * $p < 0.05$

Lower concentration of W146 was less effective in inhibiting angiogenesis

In order to test if lower concentration of W146 could also inhibit angiogenesis in a dose dependent manner, we then reduced the concentration of W146 to 1 µM. However, with lower concentration of W146, we were unable to showed significant inhibition on angiogenesis based on the metric that we used as demonstrated by skeletal length of capillary sprout in right collagen gel.

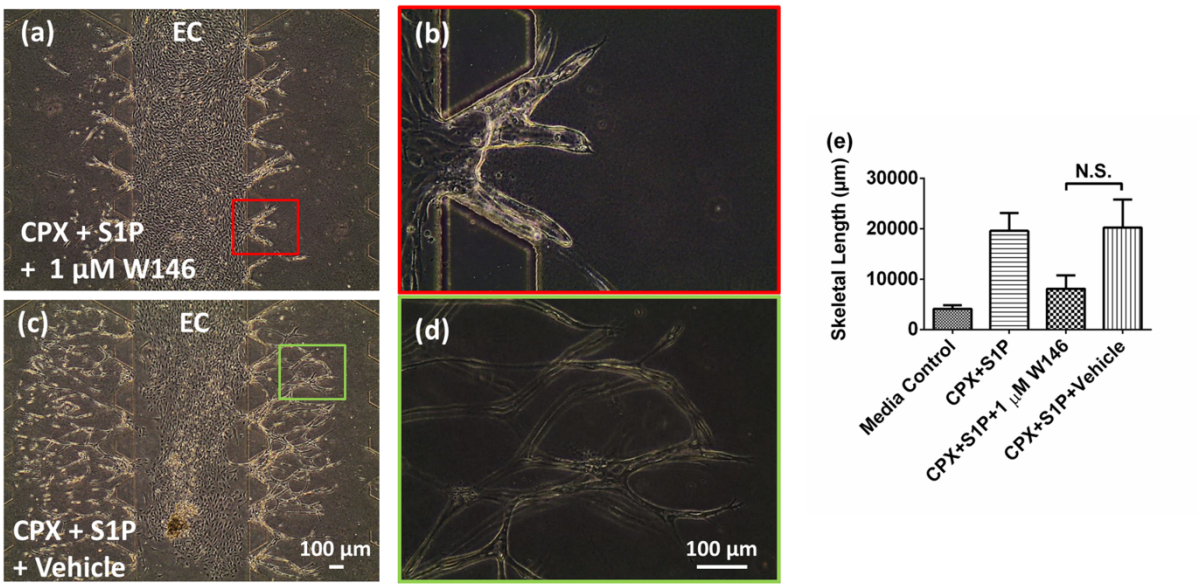

Fig. 17 Reduced concentration of W146 was less effective in inhibiting angiogenesis. (a) 4x phase contrast images of CPX + S1P induced capillary sprouting in microfluidics with 1 µM W146 or (c) equal volume of vehicle. (b) and (d) Magnified images of specified areas (marked by red and green rectangular) in (a) and (c) respectively that show detailed morphologies of sprouts in collagen gel. Some sprouts were out of focus that showed the capillary sprouting was growing across different z planes in 3D collagen gel. (e) Quantification of skeletal length under the effects of culture media, CPX + S1P, CPX + S1P + 1 µM W146 and CPX + S1P + vehicle. 1 µM of W146 did not cause significant reduction in skeletal length. Scale bar = 100 µm. Error bars denote standard error. N.S. = non-significant

S1P increases endothelial cell migration

Based on previous experiments, we observed that whenever S1P was introduced, large numbers of endothelial cells showed migrating behavior in collagen gel on the control side as compared to the treatment groups without S1P. We then quantified the number of migrating cells and migration distance on the control side to confirm if S1P increased endothelial cell migration. The quantification results were in line with qualitative comparison where S1P and CPX + S1P increased the number of migrating cells from 12.3 ± 1.7 in the media control group to 48.5 ± 6.4 and 68.8 ± 11.1, respectively. In the same context, the endothelial migration distance measured from the S1P and CPX + S1P treated groups were increased from 135 ± 21 µm in the media control group to 319 ± 14 and 327 ± 11 µm, respectively. In contrast, CPX did not influence endothelial cell migration as determined by both metrics used. Consequently, the pro-migratory effects of S1P have been confirmed in our in vitro microfluidic settings.

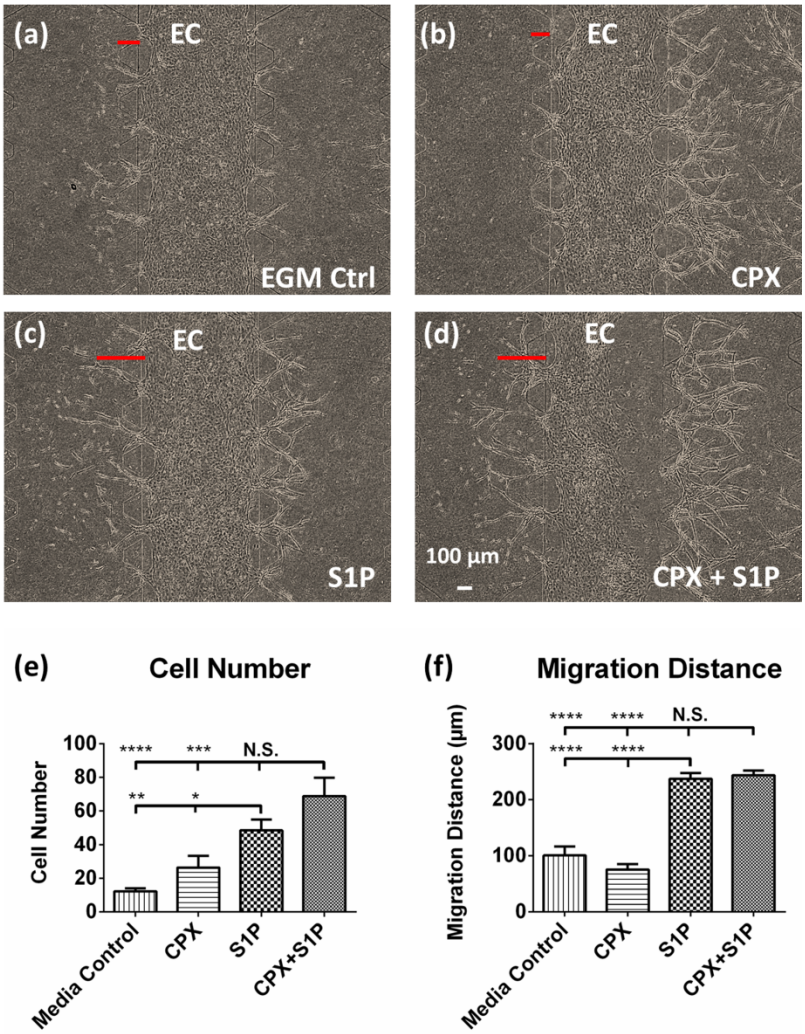

Fig. 18 S1P promotes endothelial cell migration. (a) – (d) 4x phase contrast images of endothelial cells sprouting and migrating into collagen gels under different pharmacological conditions. Endothelia migrated into collagen gel on the control side (towards empty alginate beads) of the channel. Red bars denote approximate length of migration distance. (e) – (f) Quantifications of cell number and migration distance. S1P promoted endothelia invasion into collagen gel and also increased endothelial migration distance but these effects were not seen in CPX treated groups. Scale bar = 100 μm. Error bars denote standard error. * $p < 0.05$

Calculations of active S1P in media

Murata et al. have determined the S1P concentration in both FBS and human serum which are around 100 nM and 800 nM respectively. Besides, the authors also show that the active S1P content in 10 % human serum is only 1 tenth of the total S1P content by measuring the inositol phosphate production (a process mediated by S1P receptors) [1]. By assuming the S1P activity holds true for FBS in media

Total content of S1P in media with 5 % FBS:

$$100\ nM \times 5\% = 5\ nM$$

Active S1P in media:

$$5\ nM \times 0.1 = 0.5\ nM$$

Therefore, the resulted active S1P concentration in culture media is lower than the half maximal concentration (~10 nM) needed to simulate its receptor.

Skeletal length measurement

In order to better capture the complexity of the capillary network, skeletal length of sprouts was measured. 2D projected images from 3D confocal stack images were used as the Image J plugin, AnalyzeSkeleton could accurately detect the patterns in 2D [2]. Subsequent image processing: enhancing contrast, despeckling, Gaussian blur and auto thresholding were carried out equally to all images to reduce background noise as well to prepare the images be suitable for analyzed through AnalyzeSkeleton.

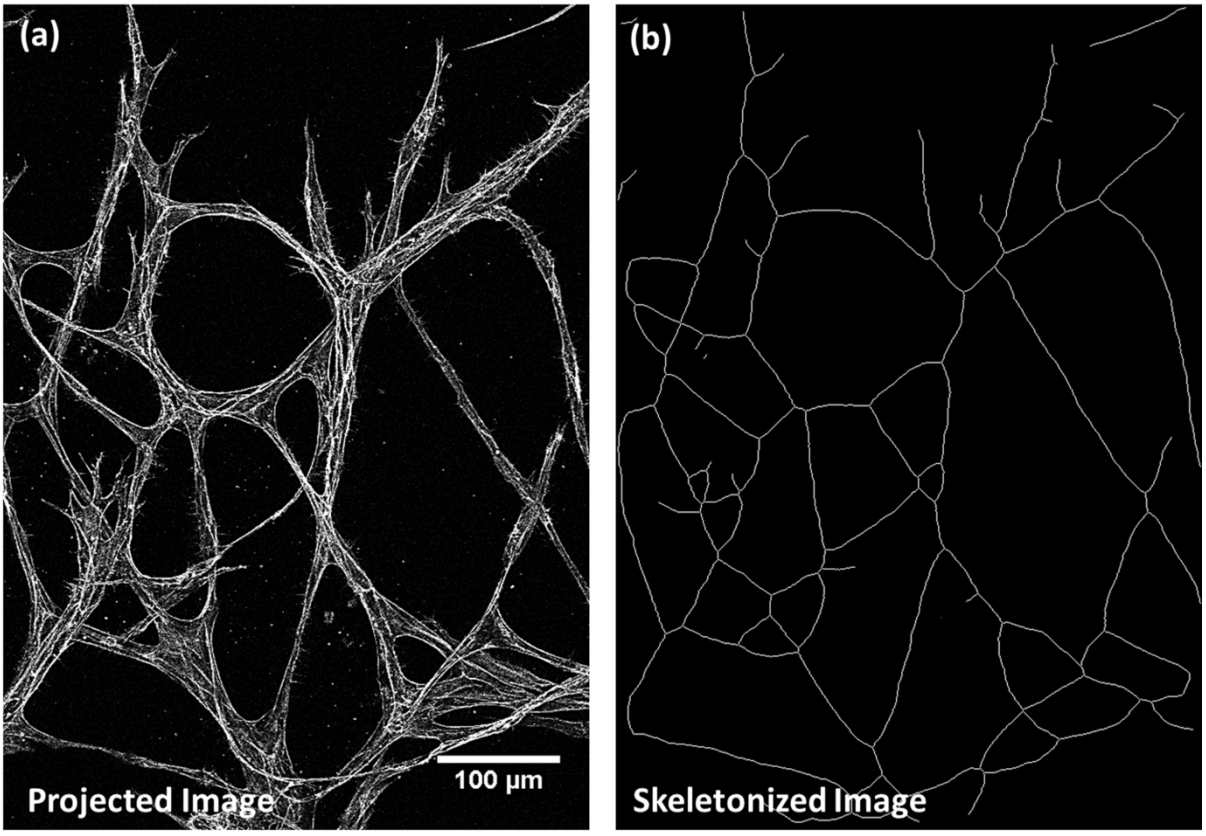

Fig. 19 Skeletal length measurement is made through skeletonizing confocal images. (a) Projected 2D image of VE-cadherin stained capillary network from 3D confocal stack images. (b) Skeletonized image of (a) by using Image J plugin, AnalyzeSkeleton. Scale bar = 100 µm.

Reference

1. N. Murata, K. Sato, J. Kon, H. Tomura, M. Yanagita, A. Kuwabara, M. Ui and F. Okajima, *Biochem J*, 2000, **352 Pt 3**, 809-815.
2. I. Arganda-Carreras, R. Fernández-González, A. Muñoz-Barrutia and C. Ortiz-De-Solorzano, *Microscopy Research and Technique*, 2010, **73**, 1019-1029.